ORIGINAL PAPER

Size, shape, and arrangement of native cellulose fibrils in maize cell walls

Shi-You Ding · Shuai Zhao · Yining Zeng

Abstract Higher plant cell walls are the major source of the cellulose used in a variety of industries. Cellulose in plant forms nanoscale fibrils that are embedded in non-cellulosic matrix polymers in the cell walls. The morphological features of plant cellulose fibrils such as the size, shape, and arrangement, are still poorly understood due to its inhomogeneous nature and the limited resolution of the characterization techniques used. Here, we sketch out a proposed model of plant cellulose fibril and its arrangement that is based primarily on review of direct visualizations of different types of cell walls in maize using atomic force microscopy at sub-nanometer scale, and is also inspired by recent advances in understanding of cellulose biosynthesis and biodegradation. We propose that the principal unit of plant cellulose fibril is a 36-chain cellulose elementary fibril (CEF), which is hexagonally shaped and 3.2 × 5.3 nm in cross-section. Macrofibrils are ribbon-like bundles containing variable numbers of CEFs associated through their hydrophilic faces. As the cell expands and/or elongates, large macrofibril may split to become smaller bundles or individual CEFs, which are simultaneously coated with hemicelluloses to form microfibrils of variable sizes during biosynthesis. The microfibrils that contain one CEF are arranged nearly parallel, and the hydrophobic faces of the CEF are perpendicular to the cell wall surface. Structural disordering of the CEF may occur during plant development while cells expand, elongate, dehydrate, and die, as well as during the processing to prepare cellulose materials.

Introduction/background

In nature, cellulose molecules, the linear β-1,4-linked glucan (polyglucose) chains, often form fibrillar structures. Depending on the degree of polymerization, the number of chains, and the way these chains pack together, the physiochemical properties of cellulose material are enormously complicated and highly variable. Knowledge of the fundamental structure of cellulose fibril is primarily gained from analyzing unusual crystals produced by algae (Nishiyama et al. 2003) and tunicates (Nishiyama et al. 2002), simply because these crystals are large enough for analysis and thus preferred for crystallography and spectroscopy. The native structure of the cellulose fibril in higher plants that accounts for the source of vast majority of cellulose material, however, remains mostly obscure. What we know about plant cellulose fibril is limited, i.e., that a number of cellulose chains

S.-Y. Ding (✉) · S. Zhao · Y. Zeng
National Renewable Energy Laboratory, Biosciences Center, Golden, CO 80401, USA
e-mail: shi.you.ding@nrel.gov

form long fibrils that are embedded in polymer matrices that are composed of hemicelluloses, pectins, and sometimes lignins. In this context, we focus on the nanoscale architecture of the plant cell walls, and thereafter use the simple term, "cellulose", which refers to the general fibrillar entity of plant cellulose. Specifically we follow our previous definitions of the terms, the cellulose elementary fibril (CEF) as the nascent fibril synthesized by the cellulose synthase rosettes, and the macrofibril as a bundle of CEFs, both contain only cellulose. The microfibril as a morphological unit often observed by microscopy may contain a single CEF or a small macrofibril, in both cases associated with hemicelluloses (Ding and Himmel 2006).

Cellulose has been investigated for more than a 100 years. Most investigations of cellulose biochemistry have been carried out by plant biologists who are particularly interested in genes, proteins and transcription factors, and their regulations of the process of plant cell wall biogenesis in a living plant. Cellulose structure, on the other hand, is assessed by chemists who are interested in properties of "purified" cellulose. The process of preparing such "pure" cellulose material usually involves the extraction of non-cellulosic polymers that co-exist with cellulose in native cell walls, such as hemicelluloses, pectins, and lignins, through the use of harsh chemicals and sometimes elevated temperature and dehydration. There is no doubt that the native structure of cellulose can be substantially altered by these purification processes.

The challenges of characterizing native plant cellulose stem mainly from three facts: (1) cellulose fibrils are small. The size of the microfibril has been reported range from 2 to 50 nm based on observations of varies microscopic and/or spectroscopic techniques (Thomas et al. 2013). However, the microfibril may be a composite structure containing multiple CEFs and hemicelluloses, the CEF and the cellulose crystallites (the contiguous regions of highly-ordered or "crystalline" cellulose found in the fibrils) are likely smaller than the apparent size of the microfibril (Nishiyama 2009; Fernandes et al. 2011). It is extremely challenging to measure such small structures by conventional high-resolution microscopy, such as TEM, without extensive sample preparation that may alter the native structure of samples in most cases. (2) The original nanostructure does not persist indefinitely. The native cellulose structure (cellulose I) is not the lowest energy state available (Simon et al. 1988). The CEFs are always associated with hemicelluloses or aggregated to form macrofibrils in native plant cell walls, transformed into more stable forms during the process of preparing cellulose materials, such as mercerized cellulose II or a mixture of crystalline and non-crystalline celluloses. (3) It is structurally inhomogeneous. The CEF is as long as several micrometers (Ding et al. 2012); disordered regions are expected in such long fibrillar structures with nanometers in dimensions. Cellulose structure may change during plant development while the cells expand, elongate, sometimes lignify, senesce, and dehydrate. Isolation of cellulose from plant materials results in shorter fibrils, further aggregation, and disordered structures. All above-mentioned factors affect data interpretation in many spectroscopic and microscopic approaches.

Despite the challenges encountered in directly visualizing cellulose structure in vivo, atomic force microscopy (AFM) is unique in its ability to image the plant cell walls either in air or under liquid, and can provide sub-nanometer resolution under certain conditions (Ding et al. 2012; Ding and Himmel 2006; Kirby et al. 1996). Although AFM is limited to imaging the surface structure, well-prepared sections can provide detailed morphological structure and arrangement of the microfibrils in the plant cell walls without extensive extraction. Our investigation is primarily based on the cell walls from naturally senescent maize, which does not necessarily represent a real native structure per se. While walls of parenchyma cells may still reserve some of the native characteristics, wood cells are nevertheless already dead as they are in living plant. In this case, wall dehydration after plant senescence may be the major concern, likely causing structural change of cellulose crystallinity (Toba et al. 2013). However, our recent study of the surface structure of parenchyma wall has demonstrated that the morphology of the microfibrils is negligibly affected in dry and re-hydrated conditions (Ding et al. 2012).

A model of the CEF

The 36-chain CEF model (Fig. 1) is primarily generated based on the hypothetic rosette structure that is
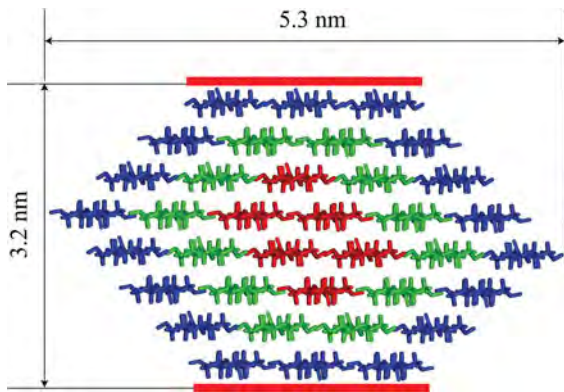
Fig. 1 Schematic model of a 36-chain cellulose elementary fibril (CEF) and the dimensions of a transverse section based on cellulose Iβ structure (Nishiyama et al. 2002). In this model, the 36 cellulose chains are arranged as a hexagonal shape in the transverse section, including two hydrophobic faces, the planar or $(1,0,0)$ and $(-1, 0, 0)$ faces, and four hydrophilic faces including the $(1, 1, 0)$, $(-1, 1, 0)$, $(1,-1,0)$, and $(-1,-1,0)$ faces. The model contains 18 surface chains (*blue*), 12 transition chains (*green*), and 6 core chains (*red*). *Red lines* highlight the two hydrophobic faces of the CEF. (Color figure online)

possibly assembled by 36 cellulose synthases (CESAs), each of them synthesizes one β-(1,4)-glucan chain (Doblin et al. 2002). Although evidences from a variety of spectroscopy have suggested smaller dimensions than 36-chain of the CEF in plants, direct visualization of maize cell walls has shown that the morphology of CEF measured by AFM appeared to be consistent with the 36-chain model (Ding and Himmel 2006; Ding et al. 2012). Here we extend our previous analysis of different types of cell walls and further compare the microfibril morphology measured by AFM with the proposed 36-chain CEF model.

Three types of cell walls

In mature plants, three types of cell walls are distinguishable under light microscopy based on their location and morphology. The primary wall (PW) is thin, non-thickened and transparent. The parenchyma-type secondary wall (pSW) is the thickened and partially lignified wall with visible lamellae as seen in parenchyma and collenchyma. The sclerenchyma-type secondary wall (sSW) is heavily thickened, elongated, and fully lignified as in sclereids, fibers, vessels, and tracheary elements. Figure 2 shows the vascular bundle area of a maize stem, in which three types of cell walls are presented.

Fig. 2 Bright field light microscopy of a transverse section of a maize stem showing the vascular bundle area containing primary cell wall (*PW*), parenchyma-type secondary cell wall (*pSW*), and sclerenchyma-type secondary cell wall (*sSW*). *ph* phloem, *v* metaxylem vessel
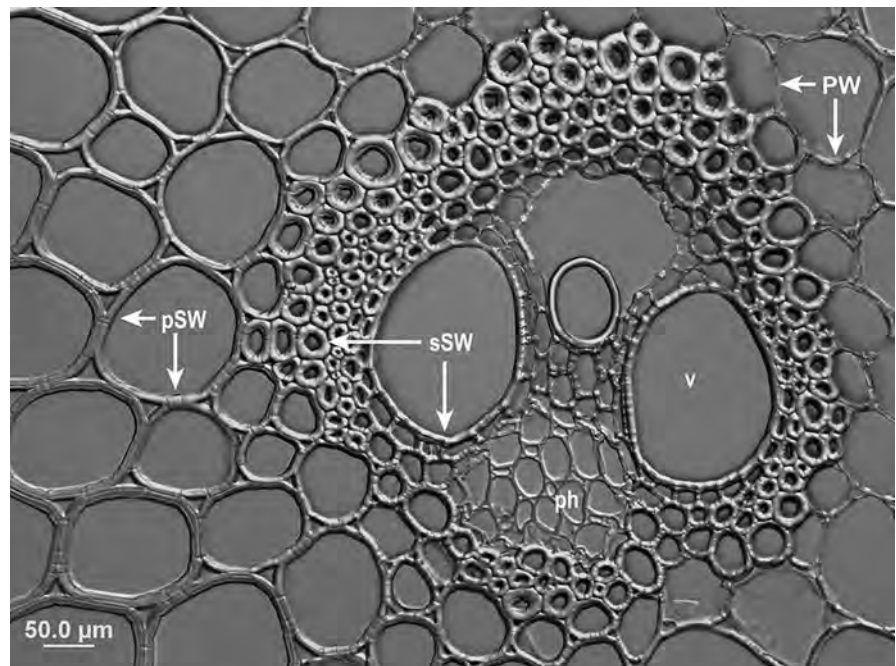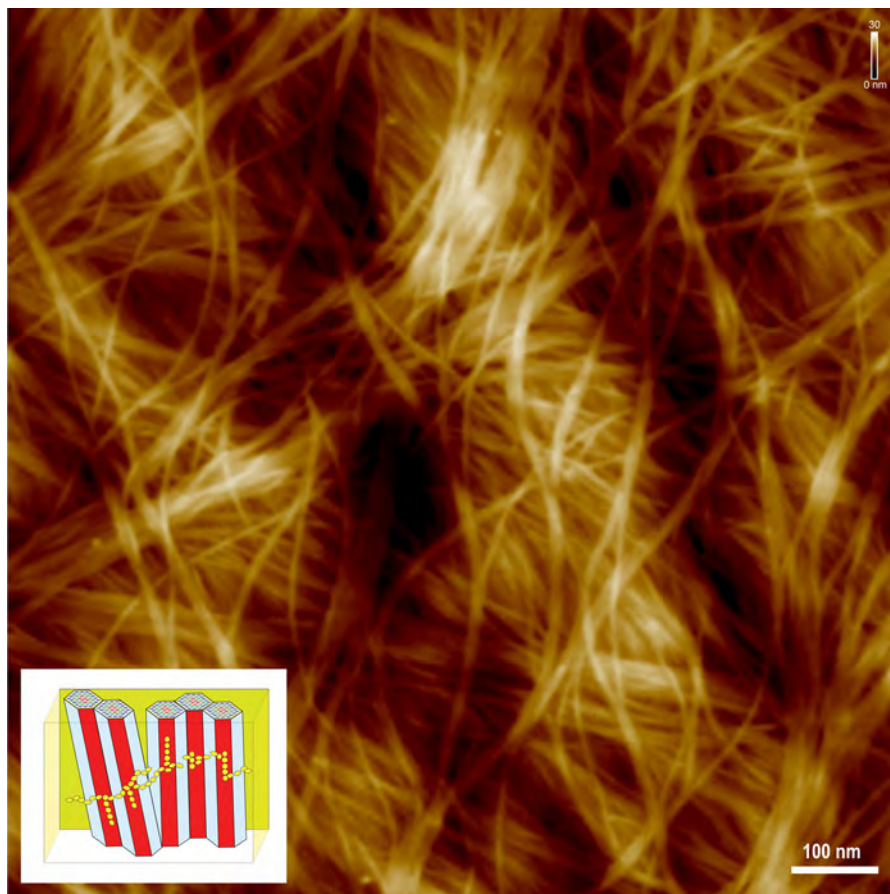
Fig. 3 Atomic force micrograph of the primary cell wall (PW) and the proposed schematic model (*insert*) showing large macrofibrils that are ribbon-like, randomly arranged, and sometimes interwoven. This representative image was taken from the parenchyma cell adjacent to the vascular bundle sheath in the maize stem (see Fig. 2)

The PW is the first wall formed when cell divides, and most differentiated cells have secondary walls (SW) that are deposited from the inner side of the PW. It has been reported that the SW deposition may commence before the cessation of cell growth (Gritsch and Murphy 2005; Macadam and Nelson 2002), which may undergo two stages, primary thickening when cell is elongating and/or expending, and secondary thickening after the cell growth ceases. Cells may have only PW or possess additionally thickened walls, i.e., pSW and sSW. Traditionally, the pSW may also be called "thickened primary wall" (Esau 1977), but the polylamellar texture of pSW is clearly different from the true PW that is thin and morphologically uniform. In this context, we define all thickened wall as SW, and the terms pSW and sSW are used to describe the primarily and secondarily thickened walls, respectively (Ding et al. 2012). It can also be noted that the PW and pSW cells are normally alive, while the sSW cells are fully lignified and dead before plant senescence. The innermost surface of the sSW is often covered by a warty layer that is formed largely from lignin precursors (Castro 1991; Ding et al. 2012; Zeng et al. 2014).

Surface structure of the cell walls

Atomic force microscopy imaging was performed in air, with the cantilever located on certain wall types with the aid of an optical microscope (Ding and Himmel 2006), which allowed us to measure the

Fig. 4 Atomic force micrograph of the parenchyma-type secondary cell wall (pSW) and the proposed schematic model (*insert*) showing parallel single CEFs and small macrofibrils in the surface. This representative image was taken from the parenchyma cell between the vascular bundles in the maize stem (see Fig. 2)
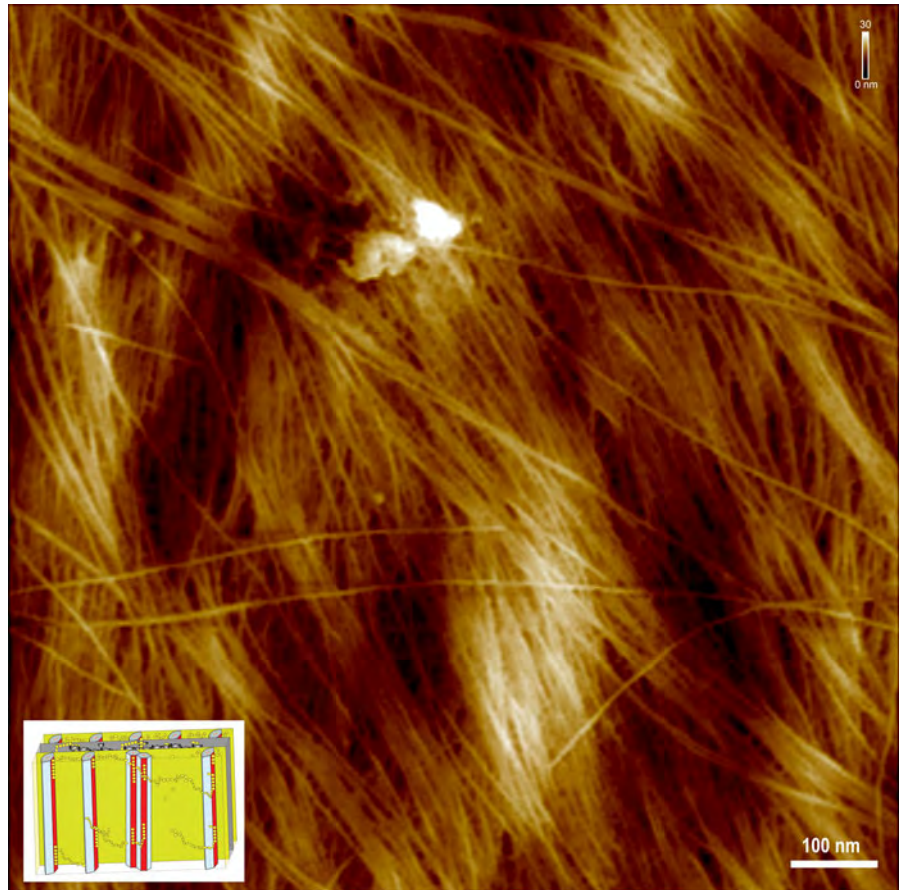
specific surface structure of the PW, pSW, and sSW. Representative AFM images are presented in Figs. 3, 4, 5. In the PW (Fig. 3), the wall surface appears to be rather clean; ribbon-like macrofibrils are predominant, which are interwoven and randomly arranged apparently containing multiple CEFs; individual CEFs are also distinguishable. The surface of pSW (Fig. 4) is also clean, similar to what observed in the PW. Most of the macrofibrils split into smaller ones and individual CEFs, and "bridges" are clearly visible that appear to be hemicelluloses. The microfibrils are arranged in nearly parallel, forming CEF-hemicellulose layers. The sSW inner surface is covered with "warts" (Fig. 5a). Microfibril structure can only be observed in wall sections. The closely packed microfibrils appear similar in size and heavily coated with matrix polymers in the sSW. Some microfibrils appear to be ribbon-like (Donaldson 2007) indicating these may contain more than one CEF (Fig. 5b).

Size, shape, and arrangement of the CEF

Clean individual CEFs and small macrofibrils can be found on the surface of pSW and PW. Occasionally the CEF is found to appear to turn 90 degrees along the long axis, which allows measurement of the fibril in different orientations. Analysis of the surface profiles suggests that the CEF is asymmetric and approximately 3 nm × 5 nm, which agrees well with the theoretical size of the 36-chain model (Fig. 6). Note that the height measurement of an individual CEF was not accurate owing to the relative rough surface of the cell wall, width measurements were used to estimate the dimensions (Ding et al. 2012). The size of the macrofibrils varies depending on the number of CEFs. Measurements of the macrofibrils containing two, three, four, and multiple CEFs are demonstrated in Figs. 6, 7, 8, 9, 10, respectively. The macrofibrils may split and the CEF may rotate from a horizontal to a
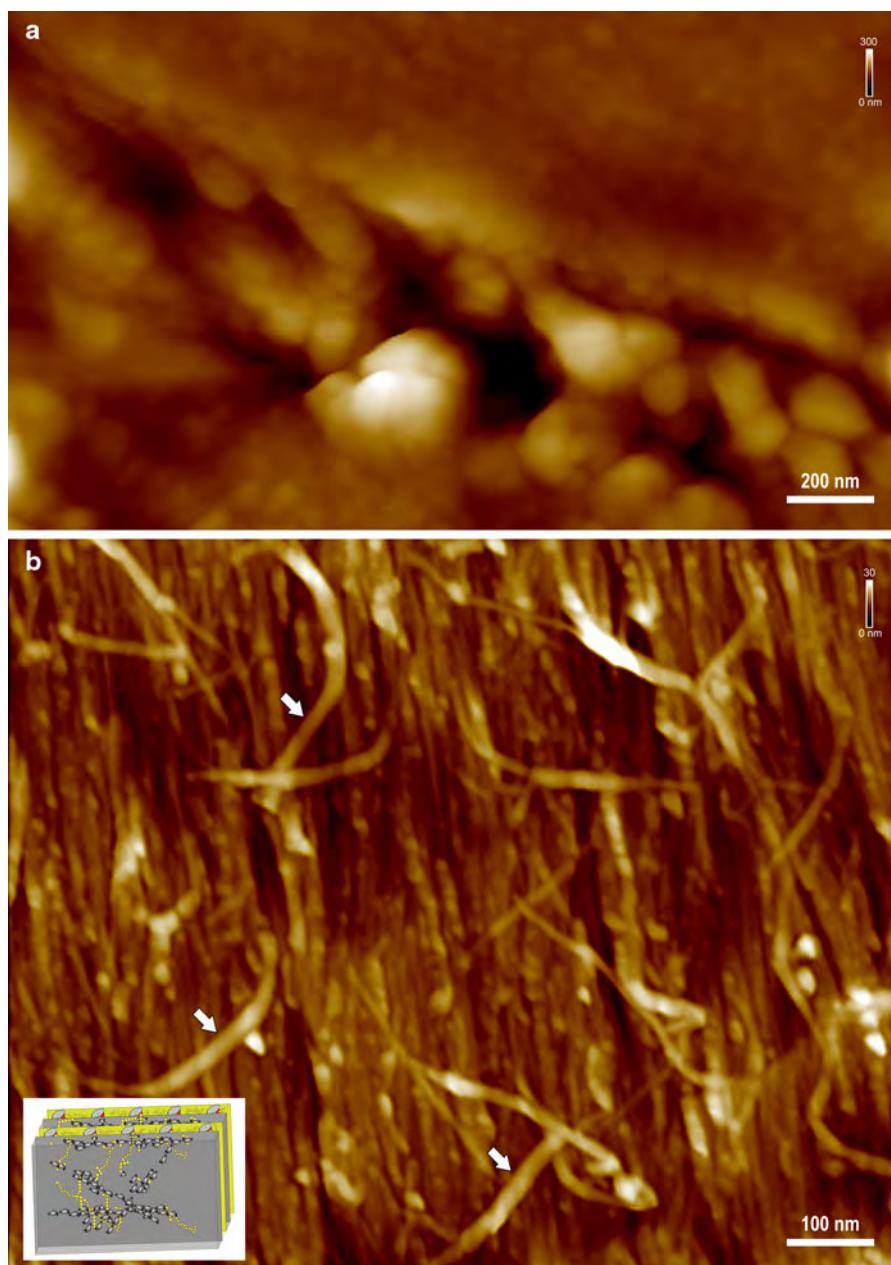
Fig. 5 Atomic force micrograph of the inner surface showing the warty layer (**a**) and a longitudinal section showing microfibrils (**b**) in the sclerenchyma-type secondary cell wall (sSW). The images were taken from the fiber cell located in the vascular bundle sheath of the maize stem (see Fig. 2). The microfibrils appear to be larger in diameter than those single CEFs observed in PW and pSW. This is probably due to hemicellulose coating. Small ribbon-like fibrils (*white arrows*) are also observed that may contain more than one CEF

vertical orientation, therefore the hydrophobic faces of the individual CEF appear to be perpendicular to the surface of the cell wall (Fig. 8). Binding (Dagel et al. 2011) of carbohydrate-binding module (CBM) that recognize specifically the hydrophobic faces of cellulose has indicated that the PW surface that primarily contains macrofibrils is highly accessible (Ding et al. 2012), suggesting that the CEFs are associated through their hydrophilic faces, forming ribbon-like macrofibrils.
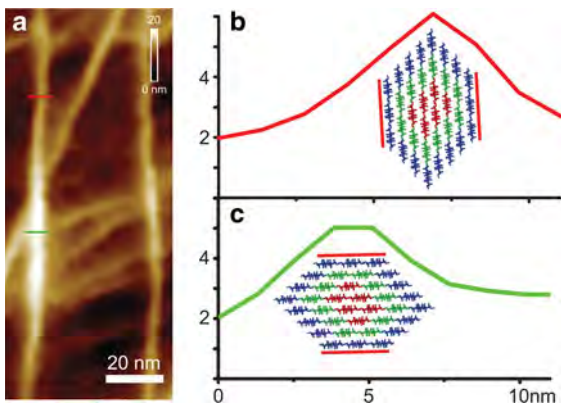
Fig. 6 Atomic force micrograph of individual CEFs (**a**), and height profiles compared with vertical (**b,** *red line* in **a**) and horizontal (**c,** *green line* in **a**) arrangements of proposed model CEF. Adapted from (Ding et al. 2012). (Color figure online)
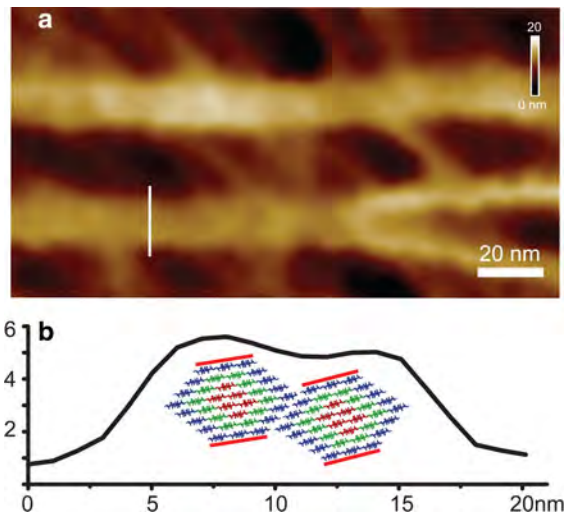
Fig. 7 Atomic force micrograph of a macrofibril that contains two CEFs (**a**) and is measured by the AFM height profile (**b,** *white line* in **a**)

Fig. 8 Atomic force micrograph of a macrofibril that contains three CEFs (**a**) and is measured by AFM height profiles before (**b,** *blue line* in **a**) and after splitting and rotating (**c,** *green line* in **a**). (Color figure online)
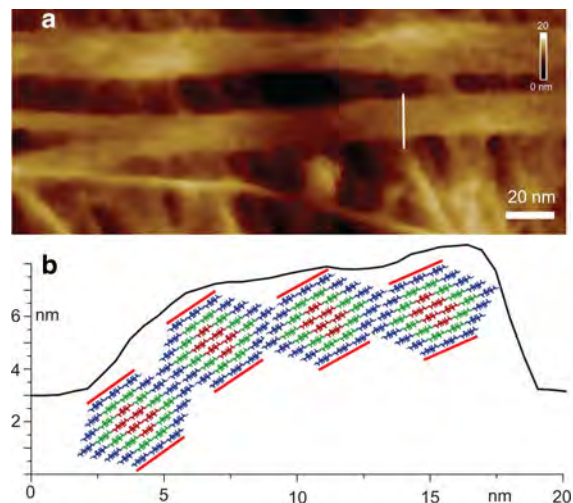
Fig. 9 Atomic force micrograph of a macrofibril that contains four CEFs (**a**) and is measured by AFM height profile (**b,** *while line* in **a**)

Discussion

Cellulose is synthesized by multiple-CESA complex. It remains unknown how many CESAs are required to form a functional cellulose synthase terminal complex or TC in different organisms. If a TC is essential to cellulose synthesis functioning and each CESA protein in the TC catalyzes synthesis of one cellulose chain, the size of the CEF will be determined by the number of CESAs in the TC. The TCs in higher plants have been observed by immune labeling and TEM techniques (Kimura et al. 1999) to be hexagonally shaped rosettes, which presumably contain 36-mer cellulose synthase isoforms and probably synthesize 36-chain CEFs (Kimura et al. 1999; Doblin et al. 2002; Ding and Himmel 2006). The CESA genes discovered in higher plants are conserved across species (Yin
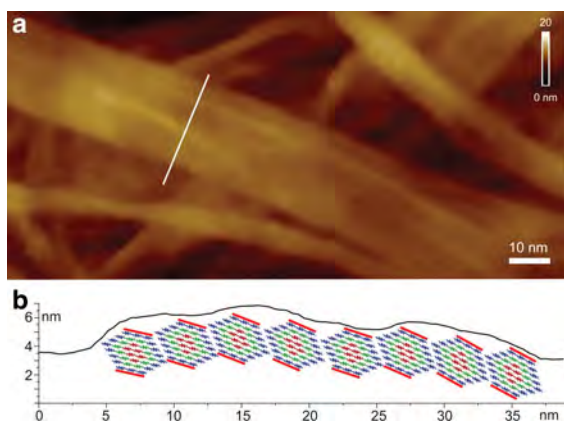
Fig. 10 Atomic force micrograph of a macrofibril that contains multiple CEFs (**a**) and is measured by AFM height profile (**b**, *white line* in **a**). The AFM image **a** is adapted from (Ding et al. 2012)

et al. 2009), which may imply that the fundamental structure of the rosettes is universal in higher plants, thereafter likely producing the same CEF.

Despite the fact that a higher order of rosettes has not been reported, direct visualization using spinning disk confocal microscopy has revealed that these rosettes are aligned with cortical microtubules (Paredez et al. 2006), which are guided by the cellulose synthesis interacting (CSI1) proteins (Li et al. 2012). We could further speculate that higher-ordered arrays of TCs, if they occur, may be dynamic and determined by cytoskeleton structure (Sampathkumar et al. 2013), a number of rosettes associated with a single microtubule may arrange as a loosely linear array. These arrayed rosettes synthesize a number of CEFs simultaneously and form ribbon-like macrofibrils as observed by AFM (Figs. 3, 4), so that the size of macrofibrils may vary in the same organism depending on the number and arrangement of the TCs in the array (Saxena and Brown 2005). The rosettes may switch between microtubules due to the traffic of the cellulose production process, resulting in interwoven macrofibrils.

The arrangement of the CEFs appears to be different in different wall types or in different layers within one wall type, which is probably the result of the process of cell expansion and/or elongation that occurs during plant development. The PW does not undergo substantial enlargement, so that the CEFs remain associated as large macrofibrils. The PW cell may exhibit limited growth driven by autonomous

changes in turgor pressure, which is normally constrained by counterforces from surrounding cells; therefore, the macrofibrils in the PW are randomly arranged. While the cell elongates, it may grow a hundred-fold larger during plant growth. During this process, the SW synthesis is accomplished by rapid deposition of cellulose and hemicelluloses, where cellulose is synthesized by an array of rosettes as the macrofibrils that then split and rotate together with associated hemicelluloses to form "sandwich-like" layers (Fig. 4) (Ding et al. 2012). Quantitative transcriptional analysis has revealed two groups of CESA genes that are differentially expressed in primary and secondary wall synthesis, respectively (Burton et al. 2004), suggesting that the rosettes may be assembled from different CESAs during secondary wall synthesis. The pSW is developed during cell growth and the sSW deposition may occur mainly after the cell has stopped increasing in size, resulting in closely packed CEFs.

Conclusions

The fibrillar structures of three types of plant cell walls (i.e., PW, pSW and sSW) were analyzed by AFM. The CEF appeared to be uniform in size in different types of walls. The dimensions of the CEF were estimated to be 3 nm x 5 nm based on the asymmetrical surface profiles of the CEF (Fig. 6), which were not inconsistent with the proposed 36-chain model that has a hexagonal cross-section. Ribbon-like macrofibrils were observed in PW and the surface of pSW, which apparently are composed of multiple CEFs associated through their hydrophilic faces. Each microfibril may contain one or multiple CEFs plus variable amounts of matrix polymer; microfibrils therefore appear dramatically different in size in different walls.

References

Burton RA, Shirley NJ, King BJ, Harvey AJ, Fincher GB (2004) The CesA gene family of barley: quantitative analysis of

transcripts reveals two groups of co-expressed genes. Plant Physiol 134(1):224–236. doi:10.1104/pp.103.032904

Castro MA (1991) Ultrastructure of vestures on the vessel wall in some species of *Prosopis* (Leguminosae–Mimosoideae). IAWA Bull 12(4):425–430

Dagel DJ, Liu YS, Zhong LL, Luo YH, Himmel ME, Xu Q, Zeng YN, Ding SY, Smith S (2011) In situ imaging of single carbohydrate-binding modules on cellulose microfibrils. J Phys Chem B 115(4):635–641. doi:10.1021/Jp109798p

Ding SY, Himmel ME (2006) The maize primary cell wall microfibril: a new model derived from direct visualization. J Agric Food Chem 54(3):597–606. doi:10.1021/jf051851z

Ding SY, Liu YS, Zeng YN, Himmel ME, Baker JO, Bayer EA (2012) How does plant cell wall nanoscale architecture correlate with enzymatic digestibility? Science 338(6110):1055–1060. doi:10.1126/science.1227491

Doblin MS, Kurek I, Jacob-Wilk D, Delmer DP (2002) Cellulose biosynthesis in plants: from genes to rosettes. Plant Cell Physiol 43(12):1407–1420. doi:10.1093/Pcp/Pcf164

Donaldson L (2007) Cellulose microfibril aggregates and their size variation with cell wall type. Wood Sci Technol 41(5):443–460. doi:10.1007/s00226-006-0121-6

Esau K (1977) Anatomy of Seed Plants. Wiley, New York

Fernandes AN, Thomas LH, Altaner CM, Callow P, Forsyth VT, Apperley DC, Kennedy CJ, Jarvis MC (2011) Nanostructure of cellulose microfibrils in spruce wood. Proc Natl Acad Sci USA 108(47):E1195–E1203. doi:10.1073/pnas.1108942108

Gritsch CS, Murphy RJ (2005) Ultrastructure of fibre and parenchyma cell walls during early stages of culm development in *Dendrocalamus asper*. Ann Bot 95(4):619–629. doi:10.1093/Aob/Mic068

Kimura S, Laosinchai W, Itoh T, Cui XJ, Linder CR, Brown RM (1999) Immunogold labeling of rosette terminal cellulose-synthesizing complexes in the vascular plant *Vigna angularis*. Plant Cell 11(11):2075–2085. doi:10.2307/3871010

Kirby AR, Gunning AP, Waldron KW, Morris VJ, Ng A (1996) Visualization of plant cell walls by atomic force microscopy. Biophys J 70(3):1138–1143

Li SD, Lei L, Somerville CR, Gu Y (2012) Cellulose synthase interactive protein 1 (CSI1) links microtubules and cellulose synthase complexes. Proc Natl Acad Sci USA 109(1):185–190. doi:10.1073/pnas.1118560109

Macadam JW, Nelson CJ (2002) Secondary cell wall deposition causes radial growth of fibre cells in the maturation zone of elongating tall fescue leaf blades. Ann Bot 89(1):89–96. doi:10.1093/aob.2002.mcf010

Nishiyama Y (2009) Structure and properties of the cellulose microfibril. J Wood Sci 55(4):241–249. doi:10.1007/s10086-009-1029-1

Nishiyama Y, Langan P, Chanzy H (2002) Crystal structure and hydrogen-bonding system in cellulose Iβ from synchrotron X-ray and neutron fiber diffraction. J Am Chem Soc 124(31):9074–9082

Nishiyama Y, Sugiyama J, Chanzy H, Langan P (2003) Crystal structure and hydrogen bonding system in cellulose Iα, from synchrotron X-ray and neutron fiber diffraction. J Am Chem Soc 125(47):14300–14306. doi:10.1021/Ja037055w

Paredez AR, Somerville CR, Ehrhardt DW (2006) Visualization of cellulose synthase demonstrates functional association with microtubules. Science 312(5779):1491–1495. doi:10.1126/science.1126551

Sampathkumar A, Gutierrez R, McFarlane HE, Bringmann M, Lindeboom J, Emons AM, Samuels L, Ketelaar T, Ehrhardt DW, Persson S (2013) Patterning and lifetime of plasma membrane localized cellulose synthase is dependent on actin organization in *Arabidopsis* interphase cells. Plant Physiol 162(2):675–688. doi:10.1104/pp.113.215277

Saxena IM, Brown RM (2005) Cellulose biosynthesis: current views and evolving concepts. Ann Bot 96(1):9–21. doi:10.1093/Aob/Mci155

Simon I, Glasser L, Scheraga HA, Manley RS (1988) Structure of cellulose.2: low-energy crystalline arrangements. Macromolecules 21(4):990–998. doi:10.1021/Ma00182a025

Thomas LH, Forsyth VT, Sturcova A, Kennedy CJ, May RP, Altaner CM, Apperley DC, Wess TJ, Jarvis MC (2013) Structure of cellulose microfibrils in primary cell walls from collenchyma. Plant Physiol 161(1):465–476. doi:10.1104/pp.112.206359

Toba K, Yamamoto H, Yoshida M (2013) Crystallization of cellulose microfibrils in wood cell wall by repeated dry-and-wet treatment, using X-ray diffraction technique. Cellulose 20(2):633–643. doi:10.1007/s10570-012-9853-7

Yin YB, Huang JL, Xu Y (2009) The cellulose synthase superfamily in fully sequenced plants and algae. BMC Plant Biol 9. doi:10.1186/1471-2229-9-99

Zeng YN, Zhao S, Yang S, Ding SY (2014) Lignin plays a negative role in the biochemical process for producing lignocellulosic biofuels. Curr Opin Biotechnol 27:38–45. doi:10.1016/j.copbio.2013.09.008